12-1-2022

Expression and localization of NRF2/Keap1 signalling pathway genes in mouse preimplantation embryos exposed to free fatty acids.

Grace Dionne
Western University

Michele D. Calder
University of Western Ontario, mcalder@uwo.ca

Dean H Betts
Western University, dean.betts@schulich.uwo.ca

Basim Abu Rafea
Western University

Andrew J Watson
Western University, awatson@uwo.ca

1 **For submission to Gene Expression Patterns- revised clean version**
2

3 **Expression and Localization of NRF2/Keap1 signaling pathway genes in mouse**
4 **preimplantation embryos exposed to free fatty acids**
5

6 Grace Dionne[1,2,3], Michele Calder[1,2,3], Dean H. Betts[1,2,3], Basim Abu Rafea[1,3], and Andrew J.
7 Watson[1,2,3]
8 [1]Department of Obstetrics and Gynaecology, [2]Department of Physiology and Pharmacology,
9 University of Western Ontario, London ON, Canada, N6A 5C1; [3]The Children's Health
10 Research Institute – Lawson Health Research Institute, London ON, Canada, N6C 2R5
11

14 Correspondence: Dr. Andrew J. Watson, Obstetrics and Gynaecology & Physiology and
15 Pharmacology, Room 257, Medical Sciences Building, University of Western Ontario, 1151
16 Richmond St, London ON, Canada, N6A 5C1; Phone: (519) 661-2111 x89132; Fax: (519) 661-
17 3721; Email: awatson@uwo.ca
18

19 Running title: Free Fatty Acids and NRF2/KEAP1 in Mouse Embryos
20

21 Key words: preimplantation embryo, obesity, infertility, palmitate, NRF2
22

23   **Abstract**

24   Obese women experience greater incidence of infertility, with reproductive tracts exposing

25   preimplantation embryos to elevated free fatty acids (FFA) such as palmitic acid (PA) and oleic

26   acid (OA). PA treatment impairs mouse preimplantation development *in vitro*, while OA co-

27   treatment rescues blastocyst development of PA treated embryos. In the present study, we

28   investigated the effects of PA and OA treatment on NRF2/ Keap1 localization, and relative

29   antioxidant enzyme (Glutathione peroxidase; *Gpx1*, Catalase; *Cat*, Superoxide dismutase; *Sod1*

30   and γ-Glutamylcysteine ligase catalytic unit; *Gclc*) mRNA levels, during *in vitro* mouse

31   preimplantation embryo development. Female mice were superovulated, mated, and embryos

32   cultured in the presence of bovine Serum albumin (BSA) control or PA, or OA, alone (each at 100

33   μM) or PA+OA combined (each at 100 μM) treatment. NRF2 displayed nuclear localization at all

34   developmental stages, whereas Keap1 primarily displayed cytoplasmic localization throughout

35   control mouse preimplantation development *in vitro*. Relative transcript levels of *Nrf2*, *Keap1*, and

36   downstream antioxidants significantly increased throughout control mouse preimplantation

37   development *in vitro*. PA treatment significantly decreased blastocyst development and the levels

38   of nuclear NRF2, while OA and PA+OA treatments did not. PA and OA treatments did not impact

39   relative mRNA levels of *Nrf2*, *Keap1*, *Gpx1*, *Cat*, *Sod1* or *Gclc*. Our outcomes demonstrate that

40   cultured mouse embryos display nuclear NRF2, but that PA treatment reduces nuclear NRF2 and

41   thus likely impacts NRF2/KEAP1 stress response mechanisms. Further studies should investigate

42   whether free fatty acid effects on NRF2/KEAP1 contribute to the reduced fertility displayed by

43   obese patients.

1. Introduction

Infertility may impact up to 1 in 6 couples worldwide (Boivin et al., 2007), and its prevalence is driving increased demand for assisted reproductive technologies (ARTs) to improve pregnancy outcomes (Sunderam et al., 2018; Chambers et al., 2021). Obese women experience higher incidence of infertility than patients with lower body mass index (Talmor & Dunphy, 2015). In 2019, 53.4% of Canadian women were either overweight or obese (Statistics Canada, 2020). The effects of maternal obesity on reproductive health include irregular menstruation, polycystic ovarian syndrome, ovulatory dysfunction, and impaired oocyte and preimplantation embryo development (ASRM, 2015; Talmor & Dunphy, 2015; Broughton & Moley, 2017). When obese women conceive, there is a higher risk of miscarriage, gestational diabetes and preeclampsia, preterm delivery, large and small for gestational age infants, and birth defects (ASRM, 2015). Obesity alters the reproductive tract environment, but while the mechanisms linking obesity to female reproductive health are not fully understood, some of the negative consequences are likely due to lipotoxicity (Broughton & Moley, 2017).

Preimplantation embryo development is the free-living period of development between oocyte fertilization and blastocyst implantation in the uterus and is commonly targeted during application of assisted reproductive technologies (ARTs) (Watson & Barcroft, 2001; Bell et al., 2008). Human and mouse embryos exhibit several morphological similarities during preimplantation development (Wamaitha & Niakan, 2018). Following insemination, as the zygote proceeds through cleavage divisions, there are waves of transcriptional activity throughout preimplantation development as the embryonic genome assumes increasing control over development (Hamatani et al., 2004; Bell et al., 2008; Wamaitha & Niakan, 2018). At the 8-cell stage, mouse blastomeres undergo compaction to form the morula, and cell lineage specification mechanisms promote inner cells into the inner cell mass (ICM; future embryonic tissue) and outer cells into the trophectoderm (TE; future extraembryonic tissue) (Chazaud & Yamanaka, 2016; Wamaitha & Niakan, 2018). Blastocyst formation, as characterized by the formation of a fluid-filled cavity then ensues and is a critical determinant of developmental competence required for initiation of pregnancy (Watson & Barcroft, 2001).

Preimplantation embryos are equipped to respond adaptively to their external environment, whether it be the reproductive tract, *in vivo* or the culture environment *in vitro* by activating several mechanisms including endoplasmic reticulum stress pathways (Abraham et al., 2012; Lin et al.,

75 2019) and antioxidant pathways (Harvey et al., 1995) regulated by numerous growth factor and

76 cytokine regulatory circuits. Obesity is associated with lipotoxicity—defined by the accumulation

77 of lipids in non-adipose tissue which can induce inflammation and cellular stress (Mota et al.,

78 2016). Obesity and elevated free fatty acids (FFAs) can increase ER stress, mitochondrial

79 dysfunction, reactive oxygen species (ROS) production and apoptosis (Furukawa et al., 2004; Wei

80 et al., 2006; Mota et al., 2016). Elevated ROS in the mouse and bovine embryo can lead to

81 developmental arrest (Guerin et al., 2001; Favetta et al., 2007).

82 Palmitic acid (PA) and oleic acid (OA) are the most abundant FFAs in human circulation

83 and the mouse reproductive tract (Jungheim et al., 2011; Abdelmagid et al., 2015; Yousif et al.,

84 2020). Excessive intracellular PA metabolism is linked to negative outcomes including ER stress,

85 apoptosis, and insulin resistance, through activation of diacylglycerol and ceramide synthetic

86 pathways (Palomer et al., 2018). High PA content in bovine follicular fluid and culture media is

87 associated with poor oocyte morphology, reduced fertilization, poorer cleavage, and blastocyst

88 development (Leroy et al., 2005; Sinclair et al., 2008; Aardema et al., 2011). In contrast,

89 intracellular OA metabolism induces triacylglycerol formation, which promotes storage in lipid

90 droplets instead of their metabolism into lipotoxic compounds such as diacylglycerol or ceramides

91 (Aardema et al., 2011; Palomer et al., 2018; Yousif et al., 2020). High OA content in follicular

92 fluid and culture media is associated with higher oocyte quality, better fertilization rates and

93 improved bovine and mouse preimplantation development (Aardema et al., 2011; Yousif et al.,

94 2020). However, it is clear there is an upper limit to this benefit of storing lipid in droplets as

95 higher levels are detrimental to porcine and bovine preimplantation development (Abe et al., 1999;

96 Kikuchi et al., 2002). We have reported that treatment with 100 μM PA *in vitro* significantly

97 reduces development of mouse embryos to the blastocyst stage and increases ER stress pathway

98 mRNAs, while co-treatment with OA reverses the negative effects of PA exposure (Yousif et al.,

99 2020).

100 Here we investigate the NF-E2 p45-related factor 2 (NRF2)/Kelch-like ECH associated

101 protein 1 (KEAP1) signalling pathway to advance our understanding of PA and OA effects during

102 mouse preimplantation development. NRF2 is a nuclear transcription factor and coordinator of

103 cytoprotective responses, including antioxidant pathways (Suzuki & Yamamoto, 2015; Huang et

104 al., 2015). NRF2 is tightly regulated at the transcriptional, translational, and post-translational

105 levels, but is primarily controlled via proteasomal degradation (Huang et al., 2015; Tonelli et al.,

106 2018). Normally, KEAP1, the primary regulatory protein of NRF2, binds to NRF2 and directs

107 ubiquitin substrate binding (Cullinan et al., 2004). Under cellular stress conditions, electrophiles

108 alter the interaction between NRF2 and KEAP1 (Huang et al., 2015). NRF2 translocates to the

109 nucleus and binds to antioxidant response elements (AREs) in the promoters of target genes

110 (Jaiswal, 2004; Suzuki & Yamamoto, 2015). Among these targets are catalase (CAT), superoxide

111 dismutase (SOD1), glutathione peroxidase (GPX1) and γ-Glutamylcysteine ligase catalytic unit

112 (GCLC) which play critical roles in metabolizing harmful oxidants from cellular environment

113 (Thimmulappa et al., 2002; Lee et al., 2003; Liu et al., 2017). These antioxidant mRNAs are

114 detectable in early mouse embryos (Harvey et al., 1995; Calder et al., 2011). NRF2/KEAP1

115 signalling is widely implicated in health and disease, protecting from oxidative stress and

116 xenobiotics, including critical role(s) in development (Kensler et al., 2007; Dong et al., 2008;

117 Huang et al., 2015; Sant et al., 2017). Activation of NRF2 is proposed as treatment for some

118 diseases including obesity (Elrashidy et al, 2020; Zhu et al., 2020), however caution should be

119 taken as activation may improve resistance of cancer cells (Sporn & Liby, 2012; Huang et al.,

120 2015).

121   The relationships between FFAs, stress response pathways, and preimplantation embryo

122 development are complex. To eventually address fertility challenges faced by obese women, it is

123 necessary to define how obesity impacts reproductive health, including the impacts of abundant

124 FFAs like PA and OA. Therefore, we have investigated a possible link between FFA treatment

125 and NRF2/KEAP1 signalling during *in vitro* mouse preimplantation embryo development. Our

126 outcomes demonstrate that PA treatment reduces nuclear NRF2 and thus likely impacts

127 NRF2/KEAP1 stress response mechanisms.

128 **2.Results**

129 **2.1 Immunolocalization of NRF2 and KEAP1 during mouse preimplantation development**

130 ***in vitro*.**

131   We first defined the NRF2/KEAP1 immunolocalization patterns throughout BSA control

132 (no PA or OA treatment) mouse preimplantation development *in vitro.* NRF2 immunofluorescent

133 protein labelling was consistently detected in the nuclei of mouse preimplantation embryos from

134 the 1-cell zygote to the blastocyst stage (**Figure 1A & B**). Blastocysts displayed a significantly

higher percentage of NRF2 positive nuclei (89.76±1.06%) compared to 4-cell embryos (72.61±4.02%; p<0.05) and 1-cell zygotes (67.92±5.80%; p<0.01). The immunolocalization pattern of NRF2 is shown in representative confocal images (**Figure 1B**). NRF2 protein immunolocalization was also detected in the cytoplasm of blastomeres from all preimplantation developmental stages, though this was not quantified.
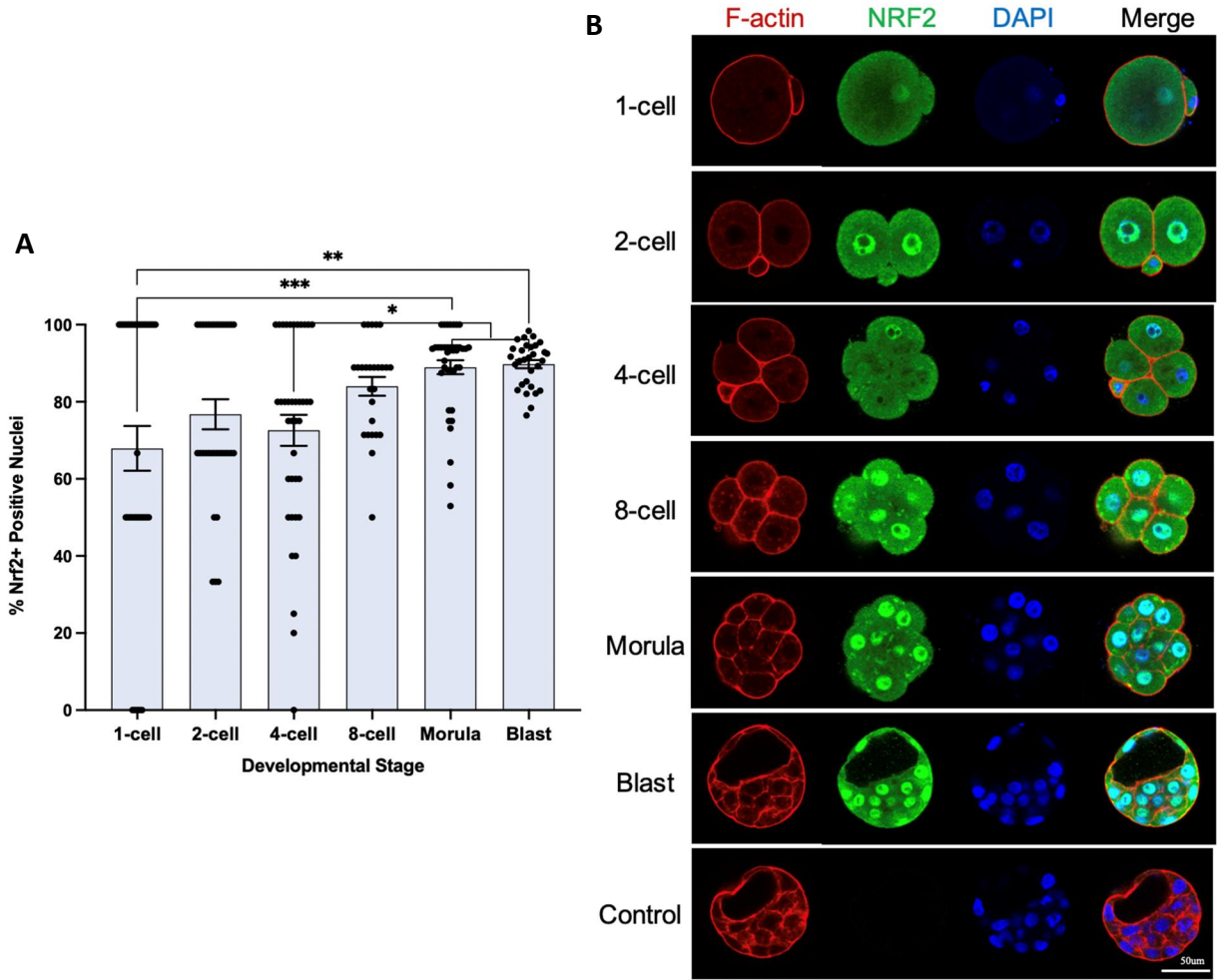

Figure 1. (A) Mean positive NRF2 nuclei (%±SEM) at each major stage of preimplantation embryo development. Nuclear NRF2 localization frequency increased throughout preimplantation embryo development, peaking at the blastocyst stage. Percentage of NRF2 positive nuclei was significantly higher at the blastocyst (89.76±1.06%) stage compared with the 1-cell (67.92±5.80%) and 4-cell stages (72.61±4.02%), per one-way ANOVA with Tukey's post-

157   hoc test (*p<0.05, **p<0.01, ***p<0.001). N=3 experimental replicates (embryo collections) with

158   a total of n=30-40 embryos measured per treatment group. **(B) Immunofluorescence images show**

159   **NRF2, F-actin and DAPI localization at each stage of preimplantation embryo development.**

160   Nuclear NRF2 localization is evident at the 1-cell, 2-cell, 4-cell, 8-cell, morula, and blastocyst

161   stages, assessed via overlap between NRF2 and DAPI. Images via Zeiss LSM 800 confocal

162   microscope. Scale bar = 50μm.

163   KEAP1 immunofluorescent localization was observed in the cytoplasm in all stages of

164   preimplantation embryo development (**Figure 2A & B**). The mean percentage of KEAP1 positive

165   cells was consistently above 90% in all embryo stages and did not differ significantly between the

166   1-cell, 2-cell, 4-cell, 8-cell, and morula groups. Thought interestingly, the percentage of KEAP1

167   positive cells was significantly lower at the blastocyst stage (91.60±1.00%) compared with the 2-

168   cell stage (97.85±1.50%). KEAP1 was immunolocalized to a small percentage of nuclei in all

169   developmental stages except the 1-cell, though this was not precisely quantified. KEAP1

170   immunofluorescence also included cytoplasmic foci, and a subcortical cytoplasmic halo in each

171   blastomere at each embryo stage **(Figure 2B)**.

172

173

174

175

176

177

178

179

180
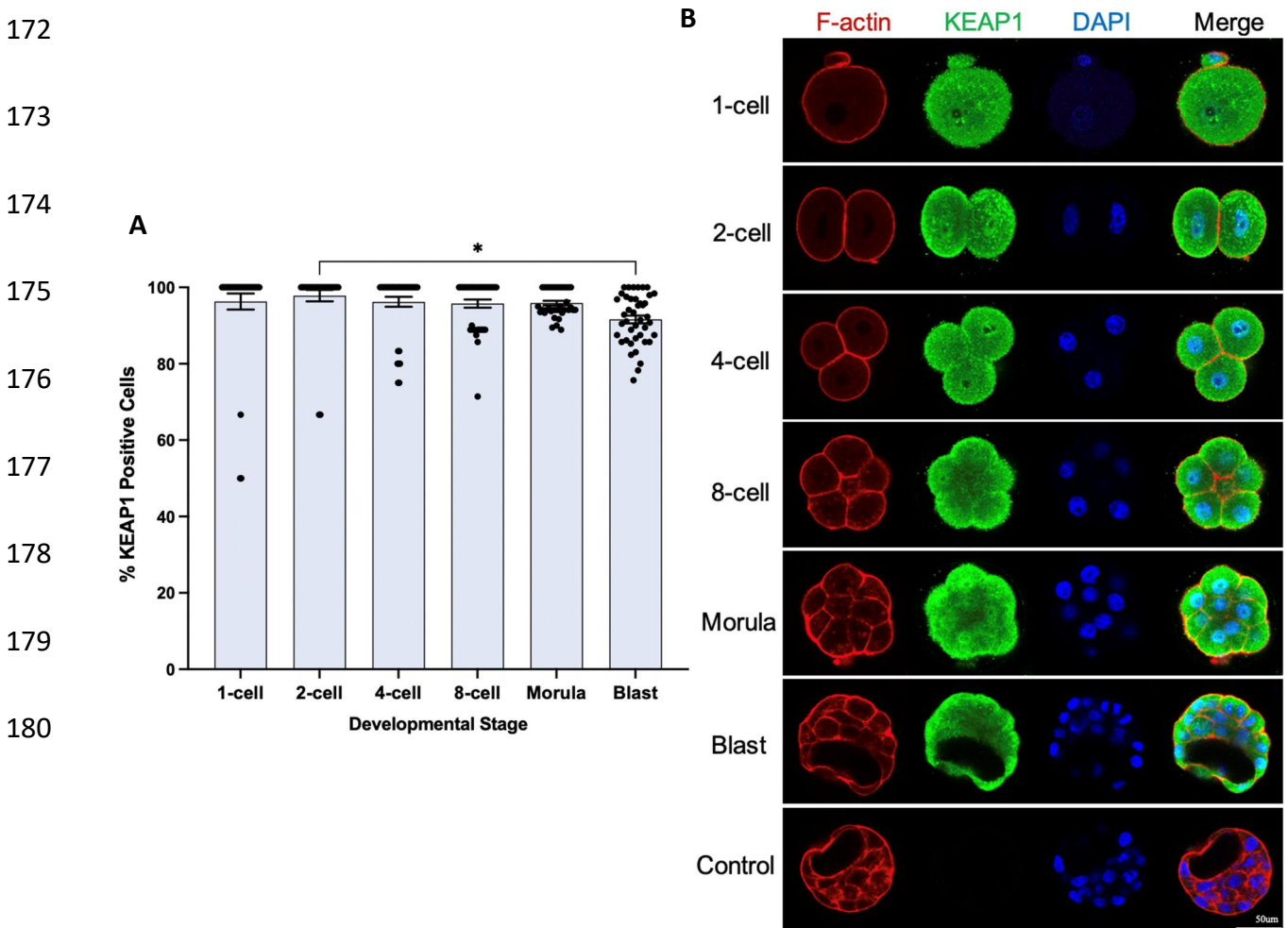
Figure 2. (A) Mean positive KEAP1 cells (%±SEM) at each stage of preimplantation embryo development. Cytosolic KEAP1 was consistently present throughout all stages of preimplantation embryo development N=3 experimental replicates (embryo collections) with a total of n=30-40 embryos measured per treatment group. Percentage of KEAP1 positive cells was significantly lower at the blastocyst stage (91.60±1.00%) compared with the 2-cell stage (97.85±1.50%). Data were analyzed using one-way ANOVA with Tukey's post-hoc test to determine significance (*$p<0.05$). **(B) Immunofluorescence images show KEAP1, F-actin and DAPI localization at each major stage of preimplantation embryo development.** Cytosolic KEAP1 presence is evident at the 1-cell, 2-cell, 4-cell, 8-cell, morula, and blastocyst stages. Scale bar = 50μm

2.2 Relative mRNA abundance of *Nrf2*, *Keap1*, and downstream antioxidants during mouse *preimplantation* development *in vitro*

We next assessed the relative abundance of NRF2/KEAP1 mRNA transcripts and selected downstream antioxidant mRNA transcripts during mouse preimplantation development *in vitro*. The relative abundance of *Nrf2* mRNA (compared to exogenously supplied luciferase mRNA; see methods) was significantly higher in blastocysts compared to the 1-cell to 8-cell stages (all $p<0.01$; **Figure 3A**), while the morula stage was intermediate. The relative mRNA abundance of *Keap1* was significantly higher in blastocysts compared to the 1-8 cell stages (all $p<0.03$; **Figure 3B**), while the morula stage did not differ from the other groups. The relative mRNA abundance of *Gpx1* significantly varied between blastocysts compared with 1-cell stage ($p<0.03$; **Figure 3C**), while the other stages were intermediate. The relative mRNA abundance of *Cat* was significantly higher in blastocysts compared with all other developmental stages (all $p<0.005$) and showed a 100-fold increase from the 1-cell stage (**Figure 3D**). The relative mRNA abundance of *Sod1* was significantly different between the blastocyst group compared with 2-cell stage only ($p<0.02$; **Figure 3E**). The relative mRNA abundance of *Gclc* was not significantly different amongst embryo stages ($p>0.19$; **Figure 3F).**
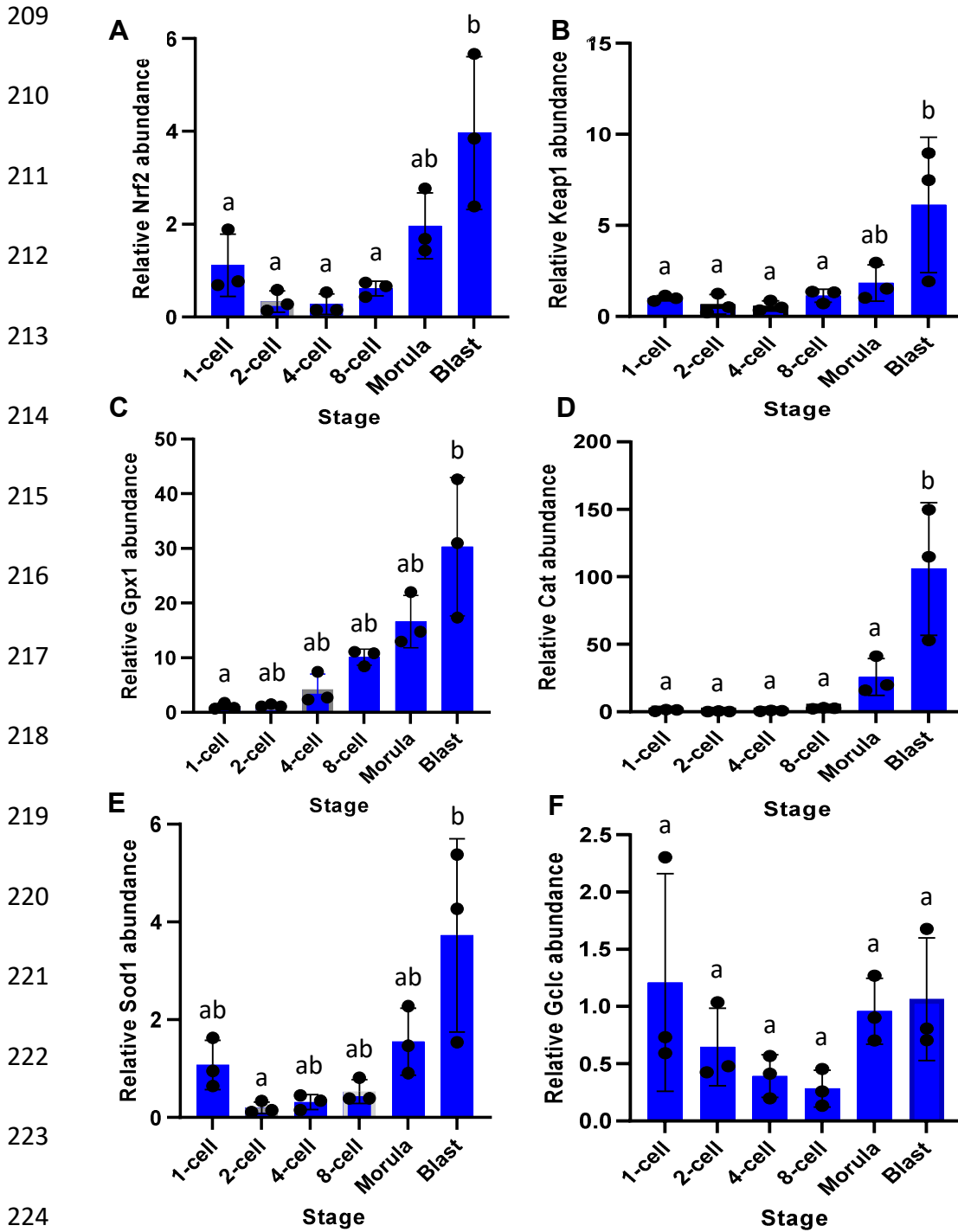
Figure 3. Mean relative mRNA abundance (±SEM) of (A) *Nrf2***, (B)** *Keap1***, (C)** *Gpx1***,**
(D) *Cat***, (E)** *Sod1* **and** *(F) Gclc* **at each stage of preimplantation embryo development.** Relative
transcript abundances (compared to exogenously supplied luciferase mRNA; see methods) of *Nrf2,*
Keap1, Gpx1, Cat, Sod1 and Gclc increase throughout mouse preimplantation embryo

development. **A**. The relative abundance of *Nrf2* mRNA (compared to exogenously supplied luciferase mRNA; see methods) was significantly higher in blastocysts compared to the 1-cell to 8-cell stages (all $p<0.01$), while the morula stage was intermediate. **B**. *Keap1* relative abundance was significantly higher in blastocysts compared to the 1-8 cell stages (all $p<0.03$), while the morula stage did not differ from the other groups. **C.** *Gpx1* relative significantly varied between blastocysts compared with 1-cell stage ($p<0.03$), while the other stages were intermediate. **D.** *Cat* relative abundance was significantly higher in blastocysts compared with all other developmental stages (all $p<0.005$) and showed a 100-fold increase from the 1-cell stage. **E.** *Sod1* relative abundance was significantly different between the blastocyst group compared with 2-cell stage only ($p<0.02$). **F.** *Gclc* was not significantly different amongst embryo stages ($p>0.19$). Relative transcript abundance in each group was compared using one-way ANOVA with Tukey's post-hoc test for *Keap1, Gclc* and *Cat*, Kruskal-Wallis non-parametric test for *Nrf2*, *Sod1* and *Gpx1* with Dunn's post-hoc test. (a,b Bars with different superscripts are significantly different, (N=3 experimental replicates each consisting of RNA extracted pools of 20 embryos for each stage; for all analyses).

2.3 Effects of PA and OA treatment on NRF2, KEAP1 protein localization during mouse preimplantation embryo development, *in vitro*

After examining untreated control *in vitro* preimplantation embryo development, we proceeded with determining the effects of PA and OA exposure on NRF2 and KEAP1 immunolocalization in a time course including 18, 24 and 48 hrs of PA, OA, and PA and OA combined treatment.

2.3.1 Localization of NRF2, KEAP1 protein after 18-hour culture with FFAs

After 18 hours of culture in the presence of BSA control, 100μM PA, 100μM OA, or 100μM PA+OA, most embryos, including those exposed to PA, 2-cell stage embryos proceeded to the 4-cell or 8-cell stage. No obvious impact of PA treatment on developmental stage was observed at this time-point (data not shown). After 18 hours of culture, nuclear NRF2 immunolocalization was present in embryos from all four treatment groups. The mean percentage

of NRF2-positive nuclei was significantly lower in PA-treated embryos (58.07±4.19%) compared with PA+OA treated embryos (73.16±3.56%; p<0.05; **Figure 4A & B**). KEAP1 immunolocalization was detected in the cytoplasm of all treatment groups at the 18-hour time-point, but the percentage of KEAP1-positive cells did not differ significantly across groups. The percentage of KEAP1-immunopositive cells was above 95% in all four treatment groups (**Figure 4C & D**). KEAP1 immunofluorescence was also observed to include a consistent subcortical cellular halo distribution in all treatment groups.
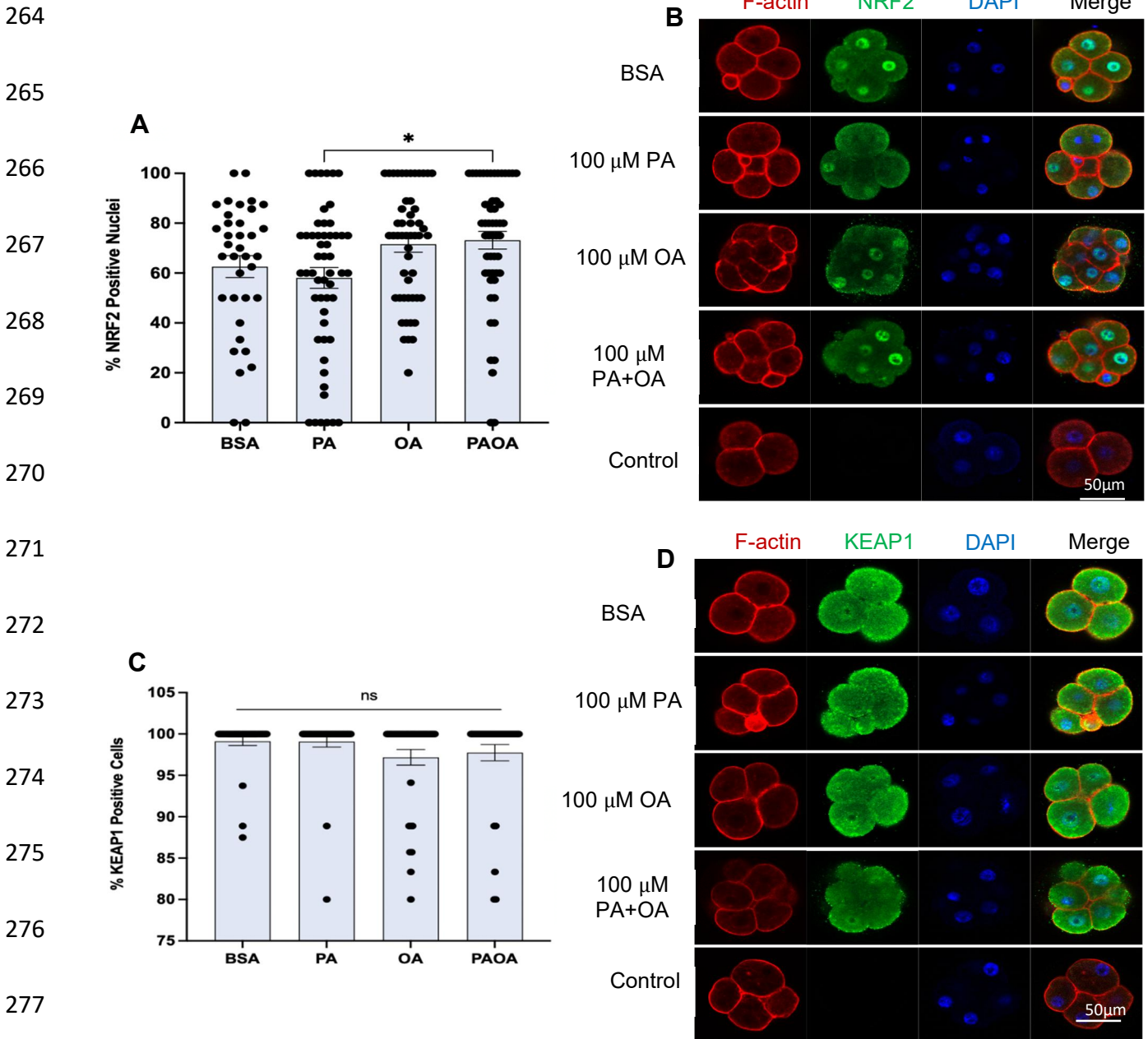
278   **Figure 4. (A) Mean positive NRF2 nuclei (%±SEM) in embryos following 18-hour culture in**

279   **BSA, PA, OA, or PA+OA treatment conditions.** Treatment with 100 μM PA significantly

280   decreased the percentage of NRF2-positive nuclei per embryo (58.07±4.19%) compared with the

281   PA+OA group (73.16±3.56%, *p<0.05). N=3 experimental replicates (embryo collections) with a

282   total of n=30-40 embryos measured per treatment group. **(B) Immunofluorescence images show**

283   **NRF2, F-actin and DAPI localization following 18-hour culture in BSA, PA, OA, or PA+OA**

284   **treatment conditions.** Nuclear NRF2 localization is evident in all treatment groups at 18 hours of

285   culture. **(C) Mean positive KEAP1 cells (%±SEM) in embryos following 18-hour culture in**

286   **BSA, PA, OA, or PA+OA treatment conditions.** Inclusion of FFA in embryo culture media did

287   not impact KEAP1 positive cells per embryo in the BSA control (99.12±0.51%), PA

288   (99.09±0.66%), OA (97.18±0.95%) and PA+OA (97.75±0.98%) groups. **(D)**

289   **Immunofluorescence images showing KEAP1, F-actin and DAPI localization following 18-**

290   **hour culture in BSA, PA, OA, or PA+OA treatment conditions.** Cytosolic KEAP1 localization

291   is evident in all treatment groups at 18 hours of culture. N=3 experimental replicates (embryo

292   collections) with a total of n=30-40 embryos measured per treatment group. Scale bars equal

293   50μm.

294

295   **2.3.2 Localization of NRF2, KEAP1 after 24-hour culture with FFAs**

296   NRF2 immunolocalization was present in the nuclei of embryos from BSA control, 100

297   μM PA, 100 μM OA, and 100 μM PA+OA after 24 hours of culture, but the frequency of NRF2-

298   positive nuclei did not differ significantly between any treatment groups (**Figure 5A & B**).

299   Cytoplasmic KEAP1 localization was observed in all treatment groups after 24 hours of culture,

300   and the mean percentage of KEAP1-positive cells did not differ significantly, while remaining

301   high (>90%) in all treatment groups (**Figure 5C & D**).

302

303

304

305

306

307

308

309

310

311

312

313

314

315

316

317

318

319

320

321

322 **Figure 5. (A) Mean positive NRF2 nuclei (%±SEM) in embryos following 24-hour culture**

323 **in BSA, PA, OA or PAOA treatment conditions.** Inclusion of FFA in embryo culture media

324 did not significantly impact the mean percentage of NRF2 positive nuclei per embryo in the BSA

325 (66.48±4.24%), PA (73.93±3.70%), OA (74.03±3.45%) and PA+OA (73.14±3.11%) groups.

326 N=3 experimental replicates (embryo collections) with a total of n=30-40 embryos measured per
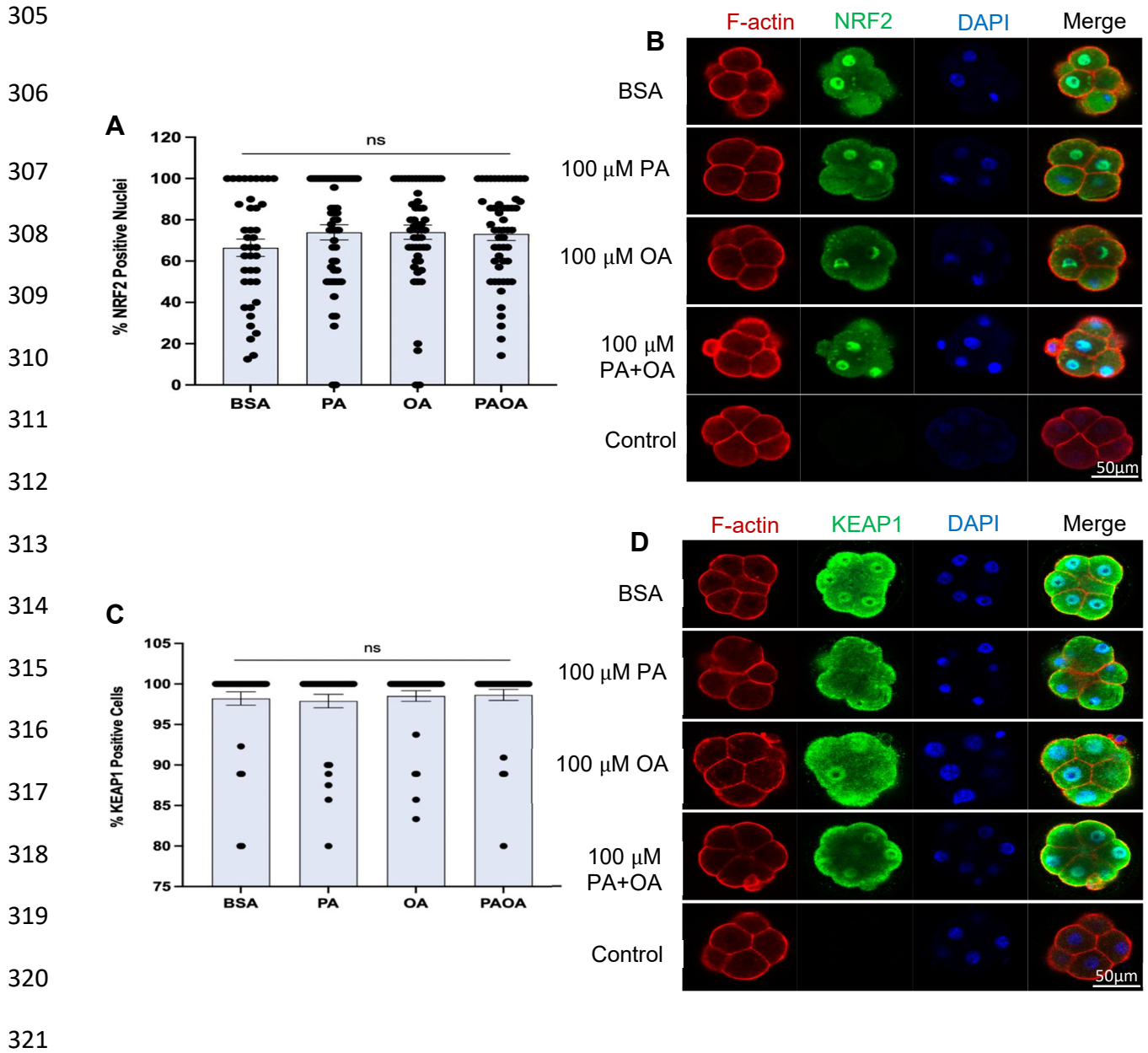
327 treatment group.

328 **(B) Immunofluorescence images showing NRF2, F-actin and DAPI localization following**

329 **24- hour culture in BSA, PA, OA or PAOA treatment conditions.** Nuclear NRF2 localization

330 is evident in all treatment groups at 24 hours of culture. **(C) Mean positive KEAP1 cells**

331 **(%±SEM) in embryos following 24-hour culture in BSA, PA, OA or PAOA treatment**

332 **conditions.** Inclusion of FFA in embryo culture media did not significantly impact the mean

333 percentage of KEAP1 positive cells per embryo in the BSA (98.21±0.81%), PA (97.89±0.83%),

334 OA (98.51±0.66%) and PA+OA (98.65±0.69%) groups. N=3 experimental replicates (embryo

335 collections) with a total of n=30-40 embryos measured per treatment group. **(D)**

336 **Immunofluorescence images showing KEAP1, F-actin and DAPI localization following 24-**

337 **hour culture in BSA, PA, OA or PAOA treatment conditions.** Cytosolic KEAP1 localization

338 is evident in all treatment groups at 24 hours of culture. Scale bars equal 50μm.

339

340 **2.3.3 Localization of NRF2, KEAP1 after 48-hour culture with FFAs**

341   NRF2 localization was present in the nuclei of embryos from BSA control, 100 μM PA,

342 100 μM OA, and 100 μM PA+OA groups after 48 hours of culture. PA exposure significantly

343 decreased the frequency of NRF2-positive nuclei (73.62±2.34%) compared with BSA control

344 (90.07±1.15%), OA (87.65±1.60%), and PA+OA (90.50±1.40%) treatment groups (p<0.0001;

345 **Figure 6A & B**). NRF2 immunofluorescence was consistently detected in the cytoplasm. KEAP1

346 displayed consistent cytoplasmic localization in embryos from all treatment groups after 48 hours

347 of culture. OA treatment alone significantly decreased the frequency of KEAP1-positive cells

348 (53.31±2.79%) compared with the BSA control (71.97±2.41%), PA (76.95±2.09%) and PA+OA

349 (86.38±1.50%) groups (p<0.0001; **Figure 6C & D**).

350

351

352

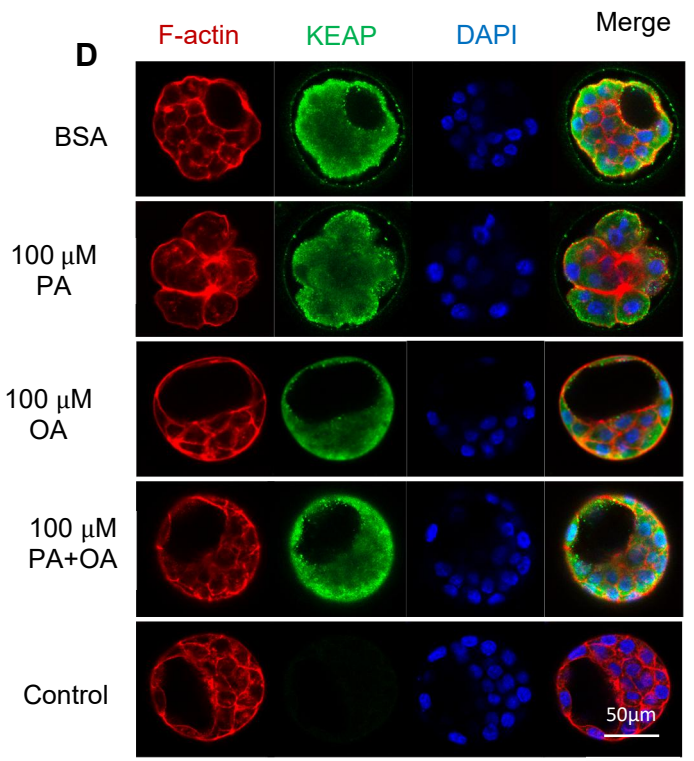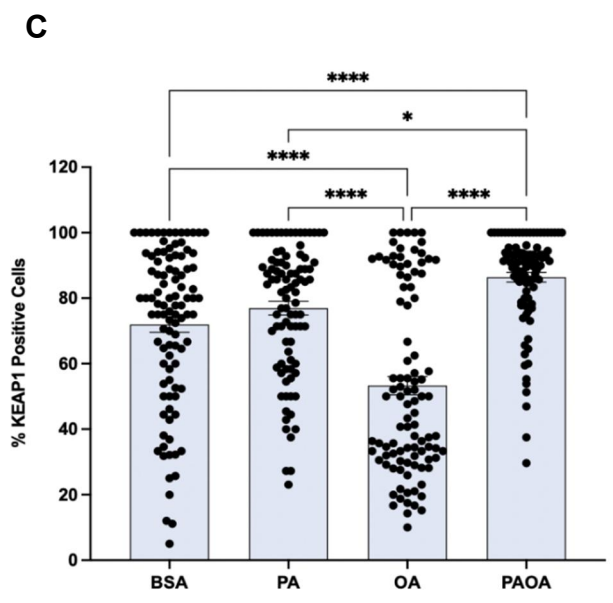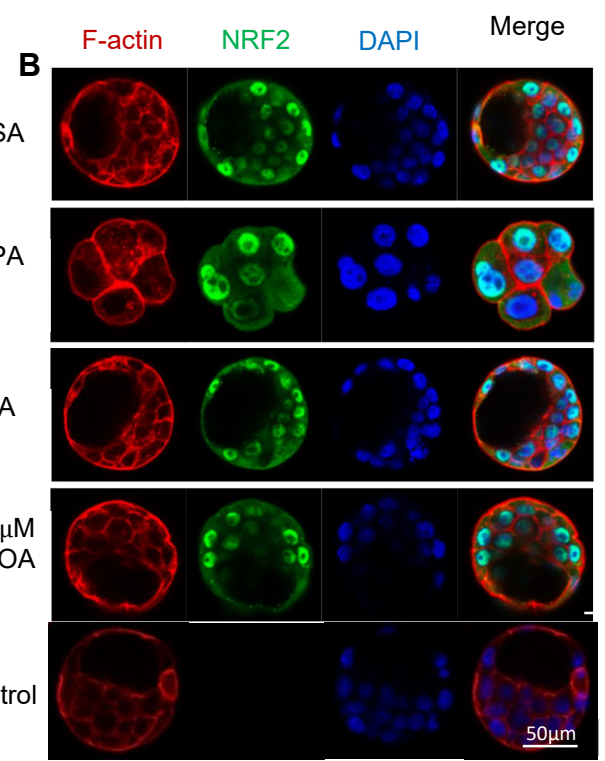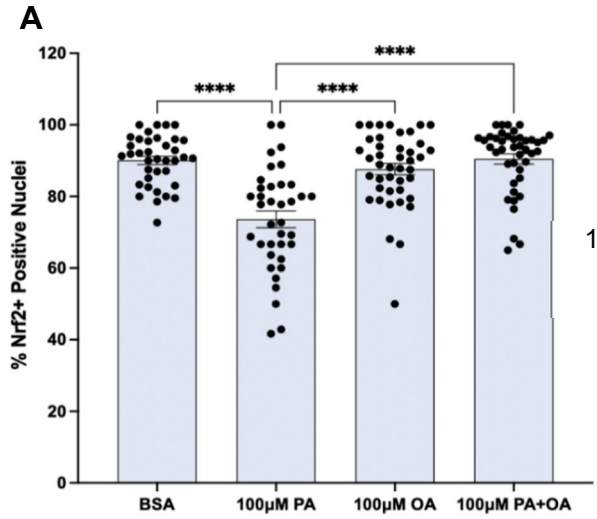
Figure 6. (A) Mean positive NRF2 nuclei (%±SEM) in embryos following 48-hour culture in BSA, PA, OA or PAOA treatment conditions. Inclusion of 100 μM PA in embryo culture media significantly decreased the percentage of positive NRF2 nuclei per embryo (73.62±2.35%) compared with BSA control (90.07±1.15%), OA (87.65±1.60%), and PA+OA (90.50±1.41%) treatments (****p<0.0001). N=3 experimental replicates (embryo collections) with a total of n=30-40 embryos measured per treatment group. **(B) Immunofluorescence images showing NRF2, F-actin and DAPI localization following 48- hour culture in BSA, PA, OA or PAOA treatment conditions.** Nuclear NRF2 localization is evident in all treatment groups. **(C) Mean positive KEAP1 cells (%±SEM) in embryos following 48-hour culture in BSA, PA, OA or PAOA treatment conditions.** Inclusion of 100 μM OA in embryo culture media significantly decreased the percentage of KEAP1 positive cells per embryo (53.31±2.79%) compared with the BSA (71.97±2.41%), PA (76.95±2.09%), and PA+OA (86.38±1.50%) treatment groups (*p<0.05, ****p<0.0001). N=3 experimental replicates (embryo collections) with a total of n=30-40 embryos measured per treatment group. **(D) Immunofluorescence images showing KEAP1, F-actin and DAPI localization following 48- hour culture in BSA, PA, OA or PAOA treatment conditions.** Cytosolic KEAP1 localization is evident in all treatment groups at 48 hours of culture. Scale bars equal 50μm.

2.4 Effects of FFA treatment on relative NRF2, KEAP1 and antioxidant mRNA levels

Lastly, we assessed the effects of PA and OA treatment on the relative abundance of NRF2, KEAP1 and the selected antioxidant enzyme mRNAs (*Gpx1, Cat, Sod1 and Gclc*). The relative abundance of *Nrf2* mRNA tended to be lower in the PA group (p>0.0535; **Figure 7A**). The relative mRNA abundance of *Keap1* was not different among treatment groups (p>0.22; **Figure 7B**). The relative mRNA abundance of *Gpx1* was not different among treatment groups (p>0.24; **Figure 7C**). The relative mRNA abundance of *Cat* tended to be lower in the PA group (p>0.11; **Figure 7D**). The relative mRNA abundance of *Sod1* was not different among treatment groups (p>0.85; **Figure 7E**). The relative mRNA abundance of *Gclc* was not significantly different among treatments (p>0.56; **Figure 7F**).
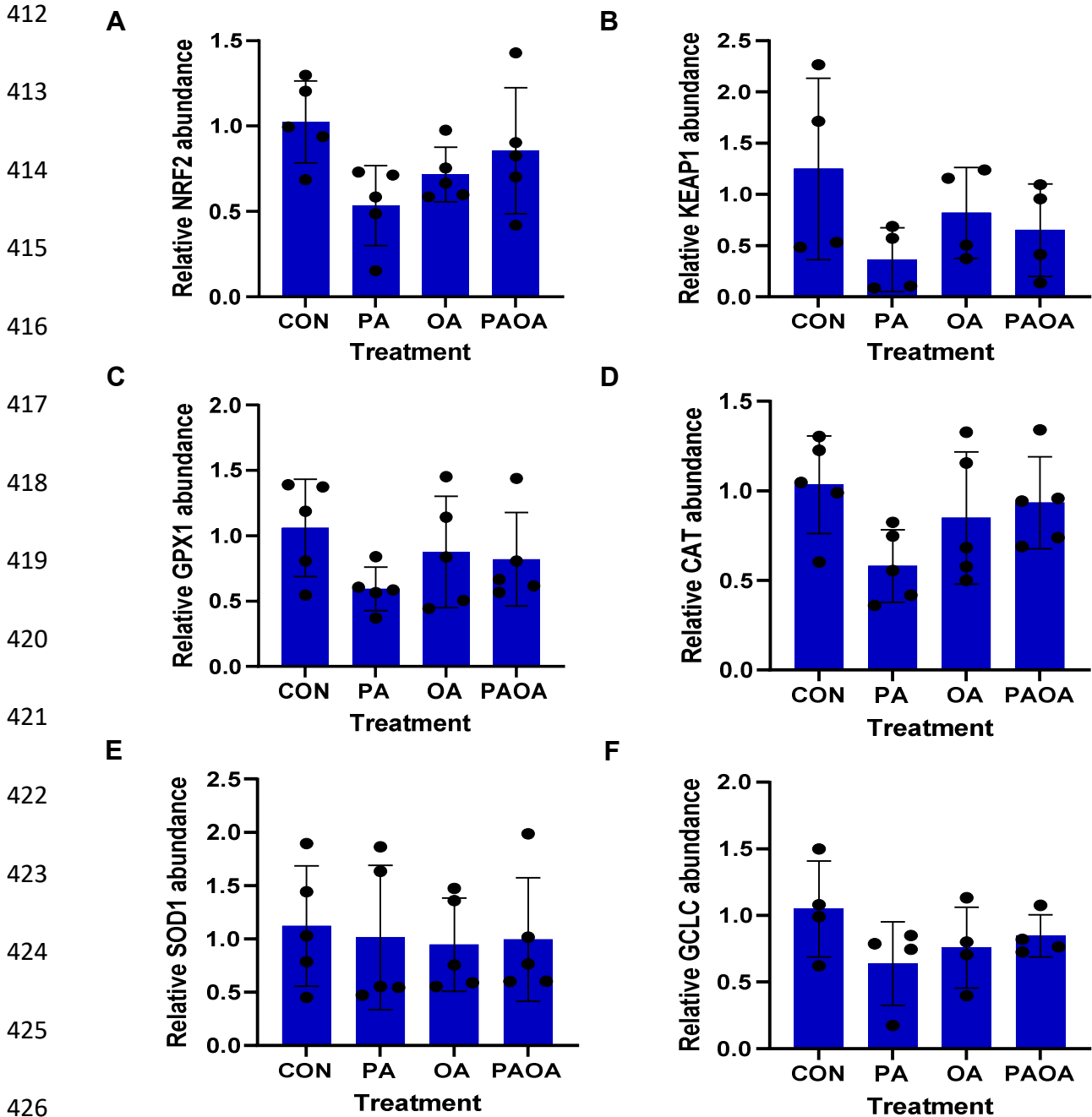
Figure 7. Mean relative mRNA abundance (±SEM) of (A) *Nrf2,* **(B)** *Keap1,* **(C)** *Gpx1,* **(D)** *Cat,* **(E)** *Sod1* **and** *(F) Gclc* **after 48h of treatment with BSA, PA, OA, or PA + OA. (A)** Relative *Nrf2* abundance tended to be lower in the PA group, $p > 0.0535$. **(B)** Relative *Keap1* abundance was not different among treatment groups, $p > 0.22$. **(C)** Relative *Gpx1* abundance was not different among treatment groups, $p > 0.24$. **(D)** Relative *Cat* abundance tended to be lower in the PA group, $p > 0.11$. **(E)** Relative *Sod1* abundance was not different among treatment groups, $p > 0.85$. **(F)**

433   Relative *Gclc* abundance was not different among treatment groups, p>0.56. Relative transcript

434   abundance in each group was compared using one-way ANOVA with Tukey's post-hoc test for

435   *Nrf2, Keap1, Gpx1* and *Cat*, Kruskal-Wallis non-parametric test for *Sod1* and *Gclc* with Dunn's

436   post-hoc test. (a,b Bars with different superscripts are significantly different). N=4 for *Keap1* and

437   *Gclc*, N=5 for *Nrf2, Gpx1, Sod1* and *Cat.*

438   **3. Discussion**

439   NRF2/KEAP1 signalling has been researched extensively as one of the dominant stress

440   response pathways in eukaryotic cells (Huang et al., 2015), and dysregulation is coincident with

441   several diseases (Kensler et al., 2007; Cuadrado et al., 2019). NRF2 is activated by oxidative and

442   ER stresses which increases NRF2 translocation into the nucleus (Cullinan et al., 2003; Kensler et

443   al., 2007). NRF2 exerts effects on downstream stress response pathways in many cell systems,

444   including antioxidant genes Gpx1, Cat, Sod1 and Gclc (Thimmulappa et al., 2002; Lee et al., 2003;

445   Liu et al., 2017). However, few studies have considered NRF2/KEAP1 signalling during

446   mammalian preimplantation development in bovine, porcine and mouse species (Amin et al., 2014;

447   Lin et al., 2018; Kim et al., 2019).

448   One of the somewhat surprising outcomes we observed was that even under the best

449   possible control mouse embryo culture conditions, NRF2 was consistently detected in the nuclei

450   at all mouse preimplantation stages, and the frequency of NRF2-positive nuclei increased as

451   preimplantation development advanced, *in vitro*. Nuclear and cytoplasmic staining of NRF2 was

452   noted in an earlier study of mouse embryos (Lin et al., 2018). However, studies in other tissues

453   suggest that NRF2 is primarily nuclear, required for basal as well as stress-mediated transcription

454   of its target genes (Nguyen et al., 2005). Embryo culture itself is a known stressor, which may

455   increase nuclear NRF2 localization (Amin et al., 2014). Amin *et al.* (2014) demonstrated that

456   embryo culture under 20% O_2 elevated *Nrf2* and antioxidant enzyme mRNA levels in bovine

457   embryos. We routinely employ a low O_2 ($5\%O_2/5\%CO_2/90\%N_2$) culture atmosphere for all

458   preimplantation mouse development culture studies as it has been demonstrated in many studies

459   to improve preimplantation development *in vitro* in several species (Meintjes et al., 2009; Wale &

460   Gardner, 2012; Amin et al., 2014; Herbemont et al., 2021) and reduce mis-regulation of embryonic

461 gene transcripts (Rinaudo et al., 2006). Therefore, nuclear NRF2 may be a component of the basal
462 mechanisms early mouse embryos employ throughout preimplantation development.

463   In contrast, KEAP1 localization was consistently detected in the cytoplasm at all stages of
464 preimplantation embryo development, and this was as is expected since KEAP1 is the cytoplasmic
465 binding partner and primary mediator of NRF2 proteasomal degradation (Watai et al., 2007;
466 Canning et al., 2015). However, cytoplasmic KEAP1 localization pattern included fluorescent foci
467 concentrated around blastomere margins. Several studies have shown that KEAP1 is associated
468 with the actin cytoskeleton (Kang et al., 2004), including focal adhesions and adherens junctions
469 (Velichkova & Hasson, 2003; Wu et al., 2018) and this is likely what is happening in early mouse
470 embryos as well. Interestingly, KEAP1 immunofluorescence localization during mouse
471 preimplantation development also included some apparent nuclear localization. Research has
472 determined that KEAP1 engages in nucleocytoplasmic shuttling to retrieve NRF2 and target it for
473 degradation (Nguyen et al., 2005).

474   The relative transcript levels of *Nrf2*, *Keap1*, *Gpx1*, *Cat* and *Sod1* all increased significantly
475 during the preimplantation period, peaking at the blastocyst stage. Mouse embryos undergo major
476 genome activations during preimplantation development that allow the embryo to shift away from
477 maternal transcripts and towards autonomous control of the embryonic genome for development
478 (Hamatani et al., 2004; Bell et al., 2008). *Gclc* mRNA was not significantly different across
479 embryo stages, in contrast to our earlier study which showed an increase in expression at the
480 blastocyst stage in a different strain of female mice (Calder et al., 2011).

481 Consistent with our previous findings, (Yousif et al., 2020), we demonstrated that treatment with
482 100 μM PA impairs mouse preimplantation development to the blastocyst stage, while co-
483 treatment with 100 μM OA rescues blastocyst development frequencies. The two non-esterified
484 fatty acids, palmitic acid (PA) and oleic acid (OA), are of particular interest because they are the
485 most abundant FFAs in plasma circulation and in the reproductive tract (Abdelmagid et al., 2015;
486 Jungheim et al., 2011). Profiling of human follicular fluid has determined that PA and OA occupy
487 approximately 27% and 31% of fatty acid content, respectively (Jungheim et al., 2011). PA is a
488 16-carbon saturated fatty acid (16:0), and OA is an 18-carbon monounsaturated fatty acid (18:1)
489 (Palomer et al., 2018). PA and OA are present at serum concentrations of approximately 100μM

490 in healthy BMI individuals, but serum levels can be elevated to anywhere between 200–400µM in

491 obese individuals (Chen et al., 2010; Colvin et al., 2017; Villa et al., 2009). Therefore, treatment

492 with concentrations of 100 µM PA and OA are consistent with serum levels found in healthy

493 pregnant women, but lower than the typical range found in obese or preeclamptic individuals

494 (Chen et al., 2010; Villa et al., 2009). Few studies have quantified FFA levels within the

495 mammalian reproductive tract, but we have reported (Yousif *et al.* 2020) reported that female CD-

496 1 mice fed a low-fat diet maintain 400 µM PA and 44 µM OA concentrations in the oviduct. Most

497 PA-treated embryos arrest at the 4- to 8-cell stages, while this does not occur in any other treatment

498 group.

499   Little is known about the effects of PA and OA on the NRF2/KEAP1 signalling pathway

500 during this developmental period. NRF2 immunofluorescence was consistently localized in the

501 nuclei of blastomeres from PA, OA, and PA+OA groups after 18, 24 and 48 hours of *in vitro*

502 treatment. The lack of significant differences between NRF2-positive nuclei in control, OA, and

503 PA+OA groups suggests two things: first, that OA likely does not affect NRF2 activation, and

504 second, that co-treatment with OA can rescue the impact of PA alone on NRF2 nuclear

505 localization. NRF2 localization outcomes at the 24-hour time-point revealed no differences

506 observed between treatment groups. Interestingly, the frequency of NRF2-positive nuclei was

507 lowest in PA-treated embryos after 18 and 48 hours. In contrast, oxidative stress upregulated

508 nuclear NRF2 in the bovine blastocyst (Amin et al., 2014). If PA induces stress, then one would

509 expect nuclear NRF2 would increase, and antioxidant expression would be stimulated in response.

510 We have previously observed that PA upregulates ER stress pathway transcripts in embryos

511 (Yousif et al., 2020), and PERK activation phosphorylates NRF2 and increases its translocation

512 into the nucleus in other systems (Cullinan et al., 2003). Paradoxically, PA treatment resulted in

513 decreased nuclear NRF2 staining in one study (Fratantonio et al., 2015). Obesity and high fat diets

514 may also decrease nuclear NRF2 and antioxidant expression (Collins et al., 2009; Elrashidy et al,

515 2020; Balasubramanian et al., 2020). NRF2 activation is suggested as a treatment for the oxidative

516 stress and inflammation of obesity and metabolic disorders (Elrashidy et al, 2020; Zhu et al., 2020).

517 Increasing NRF2 expression in PA-treated podocytes reduced oxidative and ER stress as well as

518 increased antioxidant expression and viability (Kang et al., 2021). Results from the current

519 experiments suggest that despite associated stress, PA treatment prevents preimplantation embryos
520 from properly localizing NRF2 to the nuclear compartment.

521 KEAP1 immunofluorescence was localized in the cytoplasm of blastomeres from PA, OA,
522 and PA+OA treated embryos at all time points. The frequency of cytoplasmic KEAP1 was high in
523 all groups after 18 and 24 hours, consistent with KEAP1 localization studies from other tissues
524 (Cullinan et al., 2003). After 48 hours, the frequency of cytoplasmic KEAP1 was significantly
525 lower in OA-treated embryos compared with the other treatments. In all time points, KEAP1 also
526 showed occasional nuclear localization, likely performing nucleocytoplasmic shuttling as
527 previously discussed (Nguyen et al., 2005).

528 Overproduction of ROS during embryo development may result from inadequate
529 production of antioxidants or from exposure to *in vitro* culture stresses such as high oxygen, pH,
530 light, and temperature (Lin & Wang, 2021). *Nrf2* mRNA was upregulated by oxidative stress in
531 the bovine embryo (Amin et al., 2014). *Sod1* mRNA was increased at the blastocyst stage when
532 *Nrf2* mRNA and nuclear localization of the protein increased (Amin et al., 2014). *Gclc* mRNA
533 was increased in mouse embryos cultured in high oxygen or suboptimal medium (Calder et al.,
534 2011). However, in the current study, antioxidant mRNA expression did not increase after
535 exposure to PA, which increased expression of the ER stress pathway members (Yousif et al.,
536 2020). Similarly, obesity and unhealthy metabolic state was associated with ER stress but lower
537 SOD, Catalase and GSH activity (Banuls et al., 2017; Gao et al., 2018). Zygotes from mice fed a
538 high fat diet had higher ROS and lower glutathione content (Igosheva et al., 2010). The embryo
539 may not respond appropriately to the stress of PA exposure, as NRF2 is retained within the
540 cytoplasm rather than being transported to the nucleus where it may induce expression of
541 antioxidant genes. Only embryos that developed past the 4-cell stage were used for qRT-PCR,
542 however PA-treated embryos that did not progress past this stage may not have been able to mount
543 an optimal antioxidant response.

544 This study advances our investigation into defining the differential effects of PA and OA
545 on mouse preimplantation embryo development by examining the NRF2/KEAP1 pathway. Given
546 the vulnerability of preimplantation embryo development, PA treatment at the levels investigated
547 here may have stretched the adaptive mechanisms of the developing NRF2/KEAP1 pathway,

548 resulting in impaired preimplantation development. All studies were conducted *in vitro*, but studies
549 on cultured early embryos remain important for eventual optimization of Assisted Reproductive
550 Technologies (ARTs) such as elective single embryo transfer (eSET) where culture is critical to
551 produce competent blastocysts for embryo transfer, implantation, and pregnancy.

552 **4. Experimental Procedures**

553 **4.1 Animal ethics approval**

554 All experiments used CD-1 mice sourced from Charles River Laboratories (Saint-Constant,
555 QC). Mice were handled in accordance with the Canadian Council on Animal Care, as well as
556 complying with Animal Care and Use Policies at Western University. Experiments are registered
557 to Protocol #2018-075 under Dr. Andrew J. Watson. Mice were housed in conventional housing
558 with a 12- hour light/dark cycle and access to food ad libitum (low fat diet).

559 **4.2 Mouse superovulation protocol**

560 Female CD-1 mice (4–6 weeks old) were super-ovulated by intraperitoneal (i.p.) injections
561 of 5.0 international units (IU) of pregnant mare's serum gonadotropin (PMSG, Merck Animal
562 Health, Canada) to stimulate follicular growth. 48 hours later, the same females received i.p.
563 injections of 5.0 IU of human chorionic gonadotropin (hCG, Merck Animal Health, Canada) to
564 stimulate increased ovulation. After hCG injections, female mice were placed in individual cages
565 with male CD-1 mice overnight for natural mating. For all experiments, injections were performed
566 between 10 am and noon. The morning following mating, female mice were assessed for the
567 presence of vaginal plugs which indicated successful mating.

568 **4.3 Flushing mouse embryos**

569 Only mice with seminal plugs were used to collect one-cell embryos approximately 22–24
570 hours post-hCG. Females were sacrificed using CO_2 euthanasia and dissected to isolate their
571 oviducts. Under a light microscope, the swollen portion of the oviduct was torn open to collect
572 cumulus-oocyte complexes. These were transferred to 0.03% sterile hyaluronidase in M2 medium
573 solution for 10–20 seconds to denude surrounding cumulus cells. One-cell embryos were collected

574 into 50 μL of potassium simplex optimization media with amino acids (KSOM + AA, IVL04,
575 Caisson Laboratories, Smithfield, UT), washed thrice to eliminate debris, and were then fixed for
576 immunofluorescence or frozen at -80°C for qPCR. For all other experiments, two-cell embryos
577 were collected from oviducts 46 hours post-hCG, flushed under a light microscope using warmed
578 M2 flushing medium (M7167-100, Sigma-Aldrich, Canada) in syringes with a 30g needle. After
579 washing, embryos were distributed into 20 μL treatment drops of KSOMaa under mineral oil
580 (LGOL-500, LifeGlobal Group, Guilford, CT) with up to 20 embryos in each drop under an
581 atmosphere of 5% O_2, 5% CO_2, and 90% N_2.

582 **4.4 Developmental series culture and collection of preimplantation embryos**

583 Two-cell embryos were cultured in KSOMaa drops, covered by embryo-grade mineral oil,
584 at 37°C under an atmosphere of 5% O_2, 5% CO_2, and 90% N_2. Four-cell embryos were collected
585 at approximately 18–24 hrs of culture. Eight-cell embryos were collected at approximately 24–30
586 hrs of culture. Morulae were collected at approximately 30–36 hrs of culture. Finally, blastocysts
587 were collected at approximately 48 hours of culture.

588 **4.5 Indirect immunofluorescence staining**

589 Embryo pools from each treatment group were fixed in 2% paraformaldehyde prepared in
590 PBS buffer for 30 minutes then transferred to PHEM buffer for storage at 4°C according to our
591 standard immunofluorescence protocols (Calder et al., 2011). Fixed embryos were blocked in
592 buffer consisting of: 5% normal donkey serum (017-000-121, Jackson ImmunoResearch, West
593 Grove, PA), 0.1% Triton X (EMD Millipore Corp., Billerica, MA), and 0.02% NaN3 (Sigma-
594 Aldrich) in PBS. All further washes were with antibody dilution buffer consisting of: 0.5% Normal
595 Donkey Serum, 0.05% Triton X, and 0.02% NaN3 in PBS. Embryos were incubated with either
596 anti-NRF2 antibody (#137550, Abcam, Cambridge, MA) at a dilution of 1:100 or anti-KEAP1
597 antibody (#PA5-99434, ThermoFisher) at a dilution of 1:100. Embryos were incubated in primary
598 antibodies overnight at 4°C, secondary antibody incubation with donkey anti-rabbit AlexaFluor
599 488 (711-545-152, Jackson ImmunoResearch) at a dilution of 1:400. Negative control embryos
600 were exposed to secondary antibody only. Embryos were counterstained with rhodamine-
601 phalloidin for staining filamentous actin at a dilution of 1:20 (P1951, Sigma) and 4′,6-diamidino-

602　2-phenylindole for staining nuclei at a dilution of 1:1000 (D9542, Sigma). Finally, they were

603　moved to glass-bottomed culture dishes (MatTek Life Sciences, Ashland, MA) containing two 5

604　µL drops of KSOM covered with embryo-grade mineral oil. The experiments were repeated (N=3)

605　for each primary antibody with biologically distinct embryo pools (n=30-40 embryos measured

606　per treatment group).

607　**4.6 Confocal microscopy**

608　Embryos from all treatment groups were examined using confocal microscopy with a Zeiss

609　LSM 800 AiryScan confocal microscope (Zeiss, Canada) which belongs to the Schulich Core

610　Facility. Immunofluorescence images were taken using the 10x and 25x (water) objectives. Z-

611　stacks were performed such that 10 slices of equal thickness were imaged through each embryo.

612　On the microscope, laser master gain and intensity settings were kept constant when visualizing

613　embryos from the same experiment.

614　**4.7 RNA extraction, reverse transcription and quantitative RT-PCR (qRT-PCR) to assess**

615　**relative transcript abundance**

616　Total RNA was extracted from each embryo treatment group using a PicoPure RNA

617　Isolation Kit (ThermoFisher Scientific). Exogenous luciferase mRNA (0.025 pg/embryo, Promega

618　Corporation, Fitchburg, WI) was added to each sample as a reference gene for PCR and delta delta

619　Ct analysis. DNase 1 (RNA free DNase kit, Qiagen, Toronto, ON) was used to eliminate genomic

620　DNA from embryo samples. Embryo RNA extraction pools consisted of n=20-30 embryos for

621　each treatment group and a minimum of N=3 replicate pools were assayed for each transcript of

622　interest. RNA was reverse transcribed into cDNA using SensiScript Reverse Transcriptase Kit

623　(Qiagen). cDNA was diluted to 1 embryo/µL using RNase-free water and stored at -20°C. Three

624　embryo equivalents are used per gene assayed in triplicate.

625　Quantitative PCR was performed to assess the effects of culture treatments on transcripts

626　of interest using TaqMan probes (ThermoFisher Scientific) in a 384-well plate. TaqMan primers

627　for mouse Nrf2 (#Mm00477786_m1 Nfe2l2), Keap1 (#Mm00497268_m1 KEAP1), Gpx1

628　(#Mm00656767_g1 Gpx1), Catalase (#Mm00437992_m1 Cat), Sod1 (#Mm01344233_g1 Sod1)

629　and γ-Glutamylcysteine ligase catalytic unit (Mm00802655_m1 Gclc) were used for qPCR using

630   TaqMan Gene Expression Mastermix (ThermoFisher). qRT-PCR was performed using a CFX384
631   Touch™ Real-Time PCR Detection System (BioRad, Canada). Relative transcript abundance
632   determined using the delta-delta Ct method. qRT-PCR protocols were repeated with at least (N=3)
633   biologically distinct embryo pools collected from unique batches of mice.

4.8 FFA culture treatment preparation for treatment of two-cell embryos

635   Fatty acid-free bovine serum albumin (A6003, Sigma-Aldrich, Canada), was dissolved
636   overnight in phosphate-buffered saline (PBS) to a final concentration of 20% BSA solution, then
637   filter sterilized. Stock BSA solution was used for conjugation in PA (Sigma-Aldrich, Canada) or
638   OA (Sigma-Aldrich, Canada) solution. Stock solutions were created by solubilizing PA and OA,
639   separately, in RNase-free water and sodium hydroxide (NaOH) at 70°C, to a concentration of 20
640   mM. Then, the stock solution was conjugated to BSA in a 2:1 molar ratio (PA or OA) and diluted
641   with KSOMaa to make a 500 µM solution. A similar concentration of diluted BSA without added
642   fatty acids was used for the control. Conjugated solutions were stored at 4°C for later use.

643   Treatment conditions were prepared as follows:

644   1) BSA in KSOM as the control (2 parts:3 parts KSOM v/v ratio)
645   2) 100 µM PA (1 part PA:1part BSA:3 parts KSOM v/v ratio)
646   3) 100 µM OA (1 part OA:1part BSA:3 parts KSOM v/v ratio)
647   4) 100 µM PA + 100 µM OA (1 part PA:1 part OA:3 parts KSOM v/v ratio)

4.9 Developmental stage assessment

649   At the end of the culture period in fatty acids—0 to 48 hours, depending on the
650   experiment—embryos were visually examined under a dissecting microscope at 40x to identify
651   and record their developmental stage. Embryos were categorized as being 2-cell, 4-cell, 8-cell,
652   morulae, or blastocysts. Cleavage stage embryos were identified based on the number of distinct
653   blastomeres. Morulae were identified based on the presence of compacted blastomeres and the
654   lack of a fluid-filled cavity, and blastocysts were identified as embryos with a visible fluid-filled
655   cavity. After developmental assessment, embryos were either frozen at -80°C for mRNA transcript
656   analyses or fixed for immunofluorescence labelling and confocal microscopy.

4.10 Effects of PA and OA treatment on NRF2/KEAP1 localization in preimplantation embryos

Two-cell mouse embryos were cultured in BSA control, PA, OA, or PA+OA treatments for 0 hrs, 18 hrs, 24 hrs and 48 hrs. Embryos were fixed and stained for immunofluorescence and confocal microscopy as in sections 4.5-4.6 above. Immunofluorescence images from each experiment were evaluated using FIJI (ImageJ) software. Employing Rhodamine Phalloidin and DAPI staining, the total number of cells in each embryo were counted. For NRF2 localization experiments, the number of cells with NRF2-fluorescent nuclei were counted for each embryo, defined as co-localization between the NRF2 and DAPI channels. Cell counts were used to calculate the mean percentage of NRF2-positive nuclei for each treatment. For KEAP1 localization experiments, the number of cells with KEAP1 fluorescence were counted for each embryo, defined as visual presence of KEAP1 staining inside cell boundaries. Cell counts were used to calculate the mean percentage of KEAP1-positive cells for each treatment. Cell counting for all experiments was performed using Z-stack images.

4.11 Effects of PA and OA treatment on Relative Transcript Abundance

After 48 hours of culture from the 2-cell stage, embryos of control, PA, OA and PA+OA were collected and frozen at -80°C. RNA extraction was performed as in section 4.7 above and qPCR was performed to assess the effects of culture treatments on *Nrf2*, *Keap1*, *Gpx1*, *Cat*, *Sod1* and *Gclc* mRNAs.

4.12 Statistical Analyses

GraphPad Prism 9 was used to perform all statistical analyses. For immunofluorescence imaging studies, a biological replicate was defined as a single embryo within a treatment group. For developmental assessments and qRT-PCR gene expression analyses, a biological replicate was defined as an embryo pool from a distinct group of mice. All statistical tests employed a significance threshold of $p < 0.05$. Within each treatment group, developmental stage frequency was compared using one-way analysis of variance (ANOVA) with Tukey's post-hoc test for multiple comparisons. Blastocyst frequencies were compared between treatment groups using one-way ANOVA with Tukey's post-hoc test. For immunofluorescence image analysis, percentage of

685   NRF2-positive nuclei were compared between treatment groups using one-way ANOVA with
686   Tukey's post-hoc test. Similarly, percentage of KEAP1-positive cells were compared between
687   treatment groups using one-way ANOVA with Tukey's post-hoc test. Relative mRNA abundance
688   was determined from Ct values using the delta-delta Ct method. Quantification of relative
689   transcript abundance for each gene was followed by one-way ANOVA and Tukey's post-hoc test
690   to compare between treatment groups. Where data did not pass tests for normality and equal
691   variance, a non-parametric Kruskal-Wallis test was performed with Dunn's multiple comparison
692   tests to detect differences among stages or treatments.

698   **Declaration of Competing Interests:**

699   The authors state that they have no competing interests to declare.

700

701   **Author Contributions:**

702   GD conducted all the experiments, assisted with experimental design, conducted initial
703   data analysis, and drafted the manuscript. MC assisted with embryo collection, RT-PCR data
704   collection, manuscript writing and data analysis; DHB and BaR assisted with study design, project
705   funding acquisition and editing the manuscript. AJW was principal investigator on the study,
706   oversaw study design, manuscript production and lead project funding acquisition.

707

References

1. Aardema, H., Vos, P. L. A. M., Lolicato, F., Roelen, B. A. J., Knijn, H. M., Vaandrager, A. B., Helms, B. J., & Gadella, B. M. (2011). Oleic acid prevents detrimental effects of saturated fatty acids on bovine oocyte developmental competence. *Biology of Reproduction*, 85(1), 62–69. doi: 10.1095/biolreprod.110.088815

2. Abdelmagid, S. A., Clarke, S. E., Nielsen, D. E., Badawi, A., El-Sohemy, A., Mutch, D. M., & Ma, D. W. L. (2015). Comprehensive profiling of plasma fatty acid concentrations in young healthy Canadian adults. *PLoS ONE*, 10(2), e0116195. doi: 10.1371/journal.pone.0116195

3. Abe, H., Yamashita, S., Itoh, T., Satoh, T., Hoshi, H. (1999). Ultrastructure of bovine embryos developed from in vitro-matured and -fertilized oocytes:comparative morphological evaluation of embryos cultured either in serum-free medium or in serum-supplemented medium. *Molecular Reproduction and Development* 53(3):325-35. doi: 10.1002/(SICI)1098-2795(199907)53:3<325::AID-MRD8>3.0.CO;2-T.

4. Abraham, T., Pin, C.L., Watson, A.J. (2012). Embryo collection induces transient activation of the XBP1 arm of the ER stress response while embryo vitrification does not. *Molecular Human Reproduction*, 18(5), 229-242. doi: 10.1093/molehr/gar076.

5. Amin, A., Gad, A., Salilew-Wondim, D., Prastowo, S., Held, E., Hoelker, M., Rings, F., Tholen, E., Neuhoff, C., Looft, C., Schellander, K., & Tesfaye, D. (2014). Bovine embryo survival under oxidative-stress conditions is associated with activity of the NRF2-mediated oxidative-stress-response pathway. *Molecular Reproduction and Development*, 81(6), 497-513. doi: 10.1002/mrd.22316

6. ASRM (2015). Obesity and reproduction: a committee opinion. *Fertility and Sterility* 104(5), 1116–1126. doi: 10.1016/j.fertnstert.2015.08.018

7. Balasubramanian, P., Asirvatham-Jeyaraj, N., Monteiro, R., Sivasubramanian, M.K., Hall, D., & Subramanian, M. (2020). Obesity-induced sympathetoexcitation is associated with Nrf2 dysfunction in the rostral ventrolateral medulla. *American Journal of Physiology: Regulatory, Integrative and Comparative Physiology*, 318(2), R435-R444. doi: 10.1152/ajpregu.00206.2019

8. Banuls, C., Rovira-Llopis, S., Lopez-Domenech, S., Diaz-Morales, N., Blas-Garcia, A., Veses, S., Morillas, C., Victor, V.M., Rocha, M. & Hernandez-Mijares, A. (2017). Oxidative and endoplasmic reticulum stress is impaired in leukocytes from metabolically unhealthy vs healthy obese individuals. *International Journal of Obesity*, 41(10), 1556-1563. doi: 10.1038/ijo.2017.147.

9. Bell, C.E., Calder, M.D., & Watson, A.J. (2008). Genomic RNA profiling and the programme controlling preimplantation mammalian development. *Molecular Human Reproduction* 14(12), 691-701. doi: 10.1093/molehr/gan063.

10. Boivin, J., Bunting, L., Collins, J.A., & Nygren, K.G. (2007). International estimates of infertility prevalence and treatment-seeking: potential need and demand for infertility medical care. *Human Reproduction* 22(6), 1506-1512. doi: 10.1093/humrep/dem046.

11. Broughton, D. E., & Moley, K. H. (2017). Obesity and female infertility: potential mediators of obesity's impact. *Fertility and Sterility* 107(4), 840–847. doi: 10.1016/j.fertnstert.2017.01.017

751   12. Calder, M.D, Watson, P.H., & Watson, A.J. (2011). Culture medium, gas atmosphere and
752   MAPK inhibition affect regulation of RNA-binding targets during mouse preimplantation
753   development. *Reproduction* 142, 689-698. doi: 10.1530/REP-11-0082
754   13. Canning, P., Sorrell, F. J., & Bullock, A. N. (2015). Structural basis of KEAP1
755   interactions with NRF2. *Free Radical Biology and Medicine*, 88(B), 101–107. doi:
756   10.1016/j.freeradbiomed.2015.05.034
757   14. Chambers, G.M., Dyer, S., Zegers-Hochschild, F., de Mouzon, J., Ishihara, O., Banker,
758   M., Mansour, R., Kupka, M. S., Adamson, G.D. (2021). International committee for
759   monitoring assisted reproductive technologies world report: assisted reproductive
760   technology, 2014. *Human Reproduction*, 36(11), 2921–2934. doi:
761   10.1093/humrep/deab198.
762   15. Chazaud, C., & Yamanaka, Y. (2016). Lineage specification in the mouse
763   preimplantation embryo. *Development,* 143(7), 1063–1074. doi: 10.1242/dev.128314
764   16. Chen, X., Scholl, T. O., Leskiw, M., Savaille, J., & Stein, T. P. (2010). Differences in
765   maternal circulating fatty acid composition and dietary fat intake in women with
766   gestational diabetes mellitus or mild gestational hyperglycemia. *Diabetes Care*, 33(9),
767   2049–2054. doi: 10.2337/dc10-0693
768   17. Collins, A.R., Lyon, C.J., Xia, X., Liu, J.Z., Tangirala, R.K., Yin, F., Boyadjian, R.,
769   Bikineyeva, A., Pratico, D., Harrison, D.G., & Hsueh, W.A. (2009). Age-accelerated
770   atherosclerosis correlates with failure to upregulate antioxidant genes. *Circulation*
771   *Research*, 104(6), e42-e54. doi: 10.1161/CIRCRESAHA.108.188771.
772   18. Cuadrado, A., Rojo, A.I., Wells, G., Hayes, J.D., Cousin, S.P., Rumsey, W.L., Attucks,
773   O.C., Franklin, S., Levonen, A-L., Kensler, T.W. & Dinkova-Kostova, A.T. (2019).
774   Therapeutic targeting of the Nrf2 and Keap1 partnership in chronic diseases. *Nature*
775   *Reviews Drug Discovery*, 18(4), 295-317. doi: 10.1038/s41573-018-0008-x.
776   19. Cullinan, S.B., Zhang, D., Hannink, M., Arvisais, E., Kaufman, R.J., & Diehl, J.A.
777   (2003). NRF2 is a direct PERK substrate and effector of PERK-dependent cell survival.
778   *Molecular and Cellular Biology* 23(20), 7198-7209. doi: 10.1128/MCB.23.20.7198-
779   7209.2003.
780   20. Cullinan, S. B., Gordan, J. D., Jin, J., Harper, J. W., & Diehl, J. A. (2004). The KEAP1-
781   BTB Protein Is an Adaptor That Bridges NRF2 to a Cul3-Based E3 Ligase: Oxidative
782   Stress Sensing by a Cul3-KEAP1 Ligase. *Molecular and Cellular Biology*, 24(19), 8477–
783   8486. doi: 10.1128/mcb.24.19.8477-8486.2004
784   21. Dong, J., Sulik, K.K., & Chen, S-Y. (2008). Nrf2-mediated transcriptional induction of
785   antioxidant response in mouse embryos exposed to ethanol *in vivo*: implications for the
786   prevention of fetal alcohol spectrum disorders. *Antioxidants and Redox Signaling*,
787   10(12), 2023-2033. doi: 10.1089/ars.2007.2019
788   22. Elrashidy, R.A. (2020). Dysregulation of nuclear factor erythroid 2-realted factor w
789   signaling and activation of fibrogenic pathways in hears of high fat diet-fed rats.
790   *Molecular Biology Reports*, 47(4), 2821-2834. doi: 10.1007/s11033-020-05360-3.
791   23. Favetta, L. A., St. John, E. J., King, W. A., & Betts, D. H. (2007). High levels of p66shc
792   and intracellular ROS in permanently arrested early embryos. *Free Radical Biology and*
793   *Medicine*, 42(8), 1201–1210. doi: 10.1016/j.freeradbiomed.2007.01.018
794
795

796   24. Fratantonio, D., Speciale, A., Ferrari, D., Cristani, M., Saija, A., & Cimino, F. (2015).
797   Palmitate-induced endothelial dysfunction is attenuated by cyanidin-3-O-glucoside
798   through modulation of Nrf2/Bach1 and NFκB pathways. *Toxicology Letters*, 239(3), 152-
799   160. doi: 10.1016/j.toxlet.2015.09.020.
800   25. Furukawa, S., Fujita, T., Shimabukoro, M., Iwaki, M., Yamada, Y., Nakajima,Y.,
801   Nakayama, O., Makishima, M., Matsuda, M., & Shimomura, I. (2004). Increased
802   oxidative stress in obesity and its impact on metabolic syndrome. *Journal of Clinical*
803   *Investigation* 114(12), 1752-1761. doi: 10.1172/JCI21625.
804   26. Gao, W., Du, X., Lei, L., Wang, H., Zhang, M., Wang, Z., Li, X., Liu, G., & Li, X.
805   (2018). NEFA-induced ROS impaired insulin signalling through the JNK and p38MAPK
806   pathways in non-alcoholic steatohepatitis. *Journal of Cellular and Molecular Medicine*,
807   22(7), 3408– 3422. doi: 10.1111/jcmm.13617
808   27. Guerin, P., El Mouatassim, S., & Menezo, Y. (2001). Oxidative stress and protection
809   against reactive oxygen species in the pre-implantation embryo and its surroundings.
810   *Human Reproduction Update*, 7(2), 175-189. doi: 10.1093/humupd/7.2.175.
811   28. Hamatani, T., Carter, M. G., Sharov, A. A., & Ko, M. S. H. (2004). Dynamics of Global
812   Gene Expression Changes during Mouse Preimplantation Development. *Developmental*
813   *Cell*, 6(1), 117–131. doi: 10.1016/s1534-5807(03)00373-3.
814   29. Harvey, M.B., Arcellana-Panlilio, M.Y., Zhang, X., Schultz, G.A., & Watson, A.J.
815   (1995). Expression of genes encoding antioxidant enzymes in preimplantation mouse and
816   cow embryos and primary bovine oviduct cultures employed for embryo co-culture.
817   *Biology of Reproduction* 53(3), 532-540. doi: 10.1095/biolreprod53.3.532.
818   30. Herbemont, C., Labrosse, J., Bennani-Smires, B., Cedrin-Durnerin, I., Peigne, M.,
819   Sermondade, N., Sarandi, S., Vivot, A., Vicaut, E., Talib, Z., Grynberg, M., & Sifer, C.
820   (2021). Impact of oxygen tension according to embryo stage of development: a
821   prospective randomized study. *Science Reports* 11(1), 22313. doi: 10.1038/s41598-021-
822   01488-9.
823   31. Huang, Y., Li, W., Su, Z-Y., & Kong, A-N. T. (2015). The complexity of the NRF2
824   pathway: beyond the antioxidant response. *Journal of Nutritional Biochemistry*, 26(12),
825   1401–1413. doi: 10.1016/j.jnutbio.2015.08.001
826   32. Igosheva, N., Abramov, A.Y., Poston, L, Eckert, J.J., Fleming, T.P., Duchen, M.R.,
827   McConnell, J. (2010). Maternal diet-induced obesity alters mitochondrial activity and
828   redox status in mouse oocytes and zygotes. PLoS One, 5(4), e10074.
829   doi.org/10.1371/journal.pone.0010074
830   33. Jaiswal, A.K. (2004). Nrf2 signaling in coordinated activation of antioxidant gene
831   expression. *Free Radical Biology and Medicine*, 36(10), 1199-1207. doi:
832   10.1016/j.freeradbiomed.2004.02.074.
833   34. Jungheim, E. S., Macones, G. A., Odem, R. R., Patterson, B. W., Lanzendorf, S. E.,
834   Ratts, V. S., & Moley, K. H. (2011). Associations between free fatty acids, cumulus
835   oocyte complex morphology and ovarian function during in vitro fertilization. *Fertility*
836   *and Sterility*, 95(6), 1970–1974. doi: 10.1016/j.fertnstert.2011.01.154
837   35. Kang, J.S., Son, S.S., Lee, J-H., Lee, S-W., Jeong, A.R., Lee, E.S., Cha, S-K., Chung,
838   C.H., & Lee, E-Y. (2021). Protective effects of klotho on palmitate-induced podocyte
839   injury in diabetic nephropathy. *PLoS One*, 16(4), e0250666. doi:
840   10.1371/journal.pone.0250666.

36. Kang, M-I., Kobayashi, A., Wakabayashi, N., Kim, S-G., & Yamamoto, M. (2004). Scaffolding of Keap1 to the actin cytoskeleton controls the function of Nrf2 as key regulator of cytoprotective phase 2 genes. *Proceedings of the National Academy of Sciences USA*, 101(7), 2046-2051. doi: 10.1073/pnas.0308347100.

37. Kensler, T.W., Wakabayashi, W., & Biswal, S. (2007). Cell survival responses to environmental stresses via the Keap1-Nrf2-ARE pathway. *Annual Reviews in Pharmacology and Toxicology*, 47:89-116. doi: 10.1146/annurev.pharmtox.46.120604.141046.

38. Kim, E. H., Kim, G. A., Taweechaipaisankul, A., Lee, S. H., Qasim, M., Ahn, C., & Lee, B. C. (2019). Melatonin enhances porcine embryo development via the NRF2/ARE signaling pathway. *Journal of Molecular Endocrinology*, 63(3), 175–185. doi: 10.1530/JME-19-0093

39. Kikuchi, K., Ekwell, H., Tienthai, P., Noguchi, J., Kaneko, H., Rodriguez-Martinez, H. (2002). Morphological features of lipid droplet transition during porcine oocytes fertilisation and early embryonic development to blastocyst in vivo and in vitro. *Zygote*, 10(4):355-66. doi: 10.1017/s0967199402004100.

40. Lee, J.M., Calkins, M.J., Chan, K., Kan, Y.W., & Johnson, J.A. (2003). Identification of NF-E2-related factor-2-dependent genes conferring protection against oxidative stress in primary cortical astrocytes using oligonucleotide microarray analysis. *Journal of Biological Chemistry*, 278(14), 12029-12038. doi: 10.1074/jbc.M211558200.

41. Leroy, J. L. M. R., Vanholder, T., Mateusen, B., Christophe, A., Opsomer, G., de Kruif, A., Genicot, G., & Van Soom, A. (2005). Non-esterified fatty acids in follicular fluid of dairy cows and their effect on developmental capacity of bovine oocytes in vitro. *Reproduction*, 130(4), 485–495. doi: 10.1530/rep.1.00735

42. Lin, J., & Wang, L. (2021). Oxidative stress in oocyte and embryo development: implications for in vitro systems. *Antioxidants and Redox Signaling* 34 (17), 1394-1406. doi: 10.1089/ars.2020.8209

43. Lin, T., Lee, J. E., Kang, J. W., Shin, H. Y., Lee, J. B., & Jin, D. I. (2019). Endoplasmic reticulum (ER) stress and unfolded protein response (UPR) in mammalian oocyte maturation and preimplantation embryo development. *International Journal of Molecular Sciences* 20 (2), 409. doi: 10.3390/ijms20020409

44. Lin, Y., Sui, L.-C., Wu, R.-H., Ma, R.-J., Fu, H.-Y., Xu, J.-J., Qiu, X.-H., & Chen, L. (2018). NRF2 inhibition affects cell cycle progression during early mouse embryo development. *Journal of Reproduction and Development*, 64(1), 49–55. doi: 10.1262/jrd.2017-042.

45. Liu, Y., Lu, F., Kang, L., Wang, Z., & Wang, Y. (2017). Pirfenidone attenuates bleomycin-induced pulmonary fibrosis in mice by regulating Nrf2/Bach1 equilibrium. *BMC Pulmonary Medicine*, 17(1), 63. doi: 10.1186/s12890-017-0405-7.

46. Meintjes, M., Chantilis, S.J., Douglas, J.D., Rodriguez, A.J., Guerami, A.R., Bookout, D.M., Barnett, B.D., Madden, J.D. (2009). A controlled randomized trial evaluating the effect of lowered incubator oxygen tension on live births in a predominantly blastocyst transfer program. *Human Reproduction*, 24(2), 300-307. doi: 10.1093/humrep/den368

47. Mota, M., Banini, B. A., Cazanave, S. C., & Sanyal, A. J. (2016). Molecular mechanisms of lipotoxicity and glucotoxicity in nonalcoholic fatty liver disease. *Metabolism*, 65(8), 1049–1061. doi: 10.1016/j.metabol.2016.02.014

48. Nguyen, T., Sherratt, P. J., Nioi, P., Yang, C. S., & Pickett, C. B. (2005). NRF2 controls constitutive and inducible expression of ARE-driven genes through a dynamic pathway involving nucleocytoplasmic shuttling by KEAP1. *Journal of Biological Chemistry*, 280(37), 32485–32492. doi: 10.1074/jbc.M503074200

49. Palomer, X., Pizarro-Delgado, J., Barroso, E., & Vazquez-Carrera, M. (2018). Palmitic and Oleic Acid: The Yin and Yang of Fatty Acids in Type 2 Diabetes Mellitus. *Trends in Endocrinology and Metabolism,* 29(3), 178–190. doi: 10.1016/j.tem.2017.11.009

50. Rinaudo, P.F., Giritharan, G., Talbi, S., Dobson, A.T., & Schultz, R.M. (2006). Effects of oxygen tension on gene expression in preimplantation mouse embryos. *Fertility and Sterility* 86(4 supplement), 1252-1265. doi: 10.1016/j.fertnstert.2006.05.017.

51. Sant, K. E., Hansen, J. M., Williams, L. M., Tran, N. L., Goldstone, J. V., Stegeman, J. J., Hahn, M. E., & Timme-Laragy, A. (2017). The role of Nrf1 and NRF2 in the regulation of glutathione and redox dynamics in the developing zebrafish embryo. *Redox Biology*, 13, 207–218. doi: 10.1016/j.redox.2017.05.023

52. Sinclair, K. D., Lunn, L. A., Kwong, W. Y., Wonnacott, K., Linforth, R. S. T., & Craigon, J. (2008). Amino acid and fatty acid composition of follicular fluid as predictors of in-vitro embryo development. *Reproductive BioMedicine Online*, 16(6), 859–868. doi: 10.1016/S1472-6483(10)60153-8

53. Sporn, M.B. & Liby, K.T. (2012). Nrf2 and cancer: the good, the bad and the importance of context. *Nature Reviews Cancer*, 12(8), 564-571. doi: 10.1038/nrc3278.

54. Statistics Canada (2020). Table 13-10-0373-01 Overweight and obesity based on measured body mass index, by age group and sex. doi: 10.25318/1310037301-eng

55. Sunderam, S., Kissin, D. M., Crawford, S. B., Folger, S. G., Boulet, S.L., Warner, L., & Barfield, W. D. (2018). Assisted reproductive technology surveillance - United States, 2015. *MMWR Surveillance Summaries*, 67(3), 1–28. doi: 10.15585/mmwr.ss6703a1.

56. Suzuki, T., & Yamamoto, M. (2015). Molecular basis of the KEAP1-NRF2 system. *Free Radical Biology and Medicine* 88(Part B), 93–100. doi: 10.1016/j.freeradbiomed.2015.06.006

57. Talmor, A., & Dunphy, B. (2015). Female obesity and infertility. *Best Practice and Research: Clinical Obstetrics and Gynaecology*, 29(4), 498–506. doi: 10.1016/j.bpobgyn.2014.10.014

58. Thimmulappa, R.K., Mai, K.H., Srisuma, S., Kensler, T.W., Yamamoto, M., & Biswal, S. (2002). Identification of Nrf2-regulated genes induced by the chemopreventive agent sulforaphane by oligonucleotide microarray. *Cancer Research*, 62(18), 5196-5203.

59. Tonelli, C., Chio, I. I. C., & Tuveson, D. A. (2018). Transcriptional Regulation by NRF2. *Antioxidants and Redox Signaling*, 29(17), 1727–1745. doi: 10.1089/ars.2017.7342

60. Velichkova, M., & Hasson, T. (2003). KEAP1 in Adhesion Complexes. *Cell Mobility and the Cytoskeleton*, 56(2), 109-119. doi: 10.1002/cm.10138.

61. Villa, P. M., Laivuori, H., Kajantie, E., & Kaaja, R. (2009). Free fatty acid profiles in preeclampsia. *Prostaglandins Leukotrienes and Essential Fatty Acids*, 81(1), 17–21. https://doi.org/10.1016/j.plefa.2009.05.002

62. Wale, P.L. & Gardner, D.K. (2012). Oxygen regulates amino acid turnover and carbohydrate uptake during the preimplantation period of mouse embryo development. *Biology of Reproduction* 87(1), 24, 1-8. doi: 10.1095/biolreprod.112.100552.

930 63. Wamaitha, S. E., & Niakan, K. K. (2018). Human Pre-gastrulation Development. *Current*
931   *Topics in Developmental Biology*, 128, 295–338. doi: 10.1016/B978-0-12-804252-
932   6.00012-9
933 64. Watai, Y., Kobayashi, A., Nagase, H., Mizukami, M., McEvoy, J., Singer, J.D., Itoh, K.,
934   & Yamamoto, M. (2007). Subcellular location and cytoplasmic complex status of
935   endogenous Keap1. *Genes to Cells,* 12(10), 1163-1178. doi: 10.1111/j.1365-
936   2443.2007.01118.x.
937 65. Watson, A.J., & Barcroft, L.C. (2001). Regulation of blastocyst formation. *Frontiers in*
938   *Bioscience* 6(3), D708-730. doi: 10.2741/watson.
939 66. Wei, Y., Wang, D., Topczewski, F., Pagliassotti, M.J. (2006). Saturated fatty acids
940   induce endoplasmic reticulum stress and apoptosis independently of ceramide in liver
941   cells. *American Journal of Physiology-Endocrinology Metabolism*, 291(2), E275-281.
942   doi: 10.1152/ajpendo.00644.2005.
943 67. Wu, B., Yang, S., Sun, H., Sun, T., Ji, F., Wang, Y., Xu, L., & Zhou, D. (2018). KEAP1
944   inhibits metastatic properties of NSCLC cells by stabilizing architectures of F-actin and
945   focal adhesions. *Molecular Cancer Research*, 16(3), 508–516. doi: 10.1158/1541-
946   7786.MCR-17-0544
947 68. Yousif, Maisoon D, Calder, M. D., Du, J. T., Ruetz, K. N., Crocker, K., Urquhart, B. L.,
948   Betts, D. H., Rafea, B. A., & Watson, A. J. (2020). Oleic Acid Counters Impaired
949   Blastocyst Development Induced by Palmitic Acid During Mouse Preimplantation
950   Development: Understanding Obesity-Related Declines in Fertility. *Reproductive*
951   *Sciences*, 27(11), 2038–2051. doi: 10.1007/s43032-020-00223-5
952 69. Zhu, C-G., Luo, Y., Wang, H., Li, J-Y., Yang, J., Liu, Y-X., Qu, H-Q., Wang, B-L., &
953   Zhu, M. (2020). Liraglutide ameliorates lipotoxicity-induced oxidative stress by
954   activating the NRF2 pathway in HepG2 cells. *Hormone and Metabolic Research*, 52(7),
955   532-539. doi: 10.1055/a-1157-0166.
956